LAWRENCE
LIVERMORE
NATIONAL
LABORATORY

LLNL-JRNL-640177

Analysis of Fission and Activation Radionuclides Produced by the Detonation of a Uranium-Fueled Improvised Nuclear Device and Identification of the Top Dose-Producing Radionuclides

K. Foster, T. Krauss

July 2, 2013

Health Physics

Disclaimer

Analysis of Fission and Activation Radionuclides Produced by the Detonation of a Uranium-Fueled Improvised Nuclear Device and Identification of the Top Dose-Producing Radionuclides

Terry Kraus, Sandia National Laboratory

and

Kevin Foster, Lawrence Livermore National Laboratory[†]

June 20, 2013

ABSTRACT - This paper provides the initial isotopic source term inventory of the radioactive fallout (i.e., fission and neutron-activation products) from the detonation of a uranium-fueled improvised nuclear device and identifies those radionuclides that are significant and insignificant radiological dose producers over 11 dose integration periods of interest. A primary goal of this work is to produce a set of consistent, time phase-dependent lists of the top dose-producing radionuclides for use in preparing radiological assessment calculations and data products (e.g., maps of locations exceeding protective action guidelines) by Federal Radiological Monitoring and Assessment Center Assessment Scientists and National Atmospheric Release Advisory Center scientists. Four dose pathways were analyzed to develop the lists that ranke the radionuclides by their dose contributions over the 11 time phases. The ranked-lists enable FRMAC and NARAC scientists to more quickly perform atmospheric dispersion modeling and radiological dose assessment modeling by using relatively short lists of only the top dose-producing radionuclides without significantly compromising the accuracy of the modeling and the dose projections. This paper also provides a superset-list of fallout radionuclides for the uranium-fueled device that can be used to perform radiological assessments over any desired dose time phase. Furthermore this paper provides information that may be useful to monitoring and sampling, and laboratory analysis personnel to help understand which radionuclides are of primary concern. Finally, this paper may be useful to public protection decision makers because it shows the importance of quickly initiating public protection actions to minimize the radiological dose from fallout.

Key Words: dose assessment, fission products, nuclear weapons, uranium

INTRODUCTION

The U.S. Department of Energy's National Nuclear Security Administration (NNSA) supports the Federal Radiological Monitoring and Assessment Center (FRMAC) in its mission to coordinate the federal assistance to off-site areas impacted by the release of radiological materials from accidental (e.g., nuclear power plant accident) and intentional (e.g., improvised nuclear device) incidents and to provide assistance to the Coordinating Agency responsible for the regulation and/or operation of the incident site (DOE 2010). The FRMAC is a multi-agency group that establishes the default methodologies to perform radiological assessments (SNL 2012). The FRMAC utilizes the DOE's National Atmospheric Release Advisory Center (NARAC) to provide tools and services to predict the downwind consequences of radiological material released into the atmosphere (Nasstrom et al., 2007; Sugiyama et al., 2010). Because both FRMAC and NARAC participate in the radiological assessments, this study was undertaken to ensure they use consistent source term and methods in the dose projections.

Assessing the radiological dose consequences from nuclear fallout (i.e., fission and neutron-activation products) from an IND is a difficult and complex process because of the large number (greater than 1,000) of radionuclides produced by fission and neutron activation processes. Current atmospheric dispersion models and dose assessment models cannot assess this large number of radionuclides in the period of time required to meet emergency response needs. Many of the fallout radionuclides produce negligible dose over various time periods of interest because of their characteristic radiation emissions, decay chains and radiological decay half-lives. Identifying the radionuclides in the fallout inventory that contribute the majority of the dose and those that contribute insignificant dose provides useful information. The significant advantage of developing time-phase dependent lists of only the top dose-producing radionuclides from a uranium-fueled IND is that these shorter lists enable atmospheric dispersion modeling and radiological assessment modeling to be performed much more efficiently without significantly compromising the accuracy of the results. In addition, identifying the top dose-producing radionuclides also helps direct monitoring, sampling and laboratory analysis efforts in support of the response to an IND detonation because their efforts should concentrate on identifying the top dose-producing radionuclides. Understanding the significant radiological dose pathways and the rate at which the radiological dose is delivered provides useful information to decision makers to help them initiate the appropriate public protection decisions.

BACKGROUND

In preparation for National Level Exercise (NLE) 2010, a subgroup of the FRMAC Assessment Working Group (AWG) developed default radionuclide mixture lists of the highest dose-contributing nuclides from nuclear fallout over various time phases. These lists were developed using the published lists of approximately 200 calculated fission and neutron-activation product areal activities (MBq m^{-2}) as a function of time (Hicks 1985). Although these top dose-producing radionuclide lists were informative and useful they had the following limitations:

- The Hicks radionuclide inventory data essentially started at 12 hours post detonation, and therefore, did not include the dose from the short-lived radionuclides that decayed away into daughter radionuclides or stable nuclides during the first 12 hours following the detonation. Therefore, it was not possible to perform a complete dose reconstruction during the early hours after detonation because the radionuclide inventory provided by Hicks is not complete.
- The Hicks data does not include the initial (detonation time) source strengths of the fission and neutron activation radionuclides that are required for use in NARAC modeling.

This investigation was undertaken to address the limitations described above and to develop more accurate time phase-dependent lists of the dominant dose-producing radionuclides from an IND detonation for use by FRMAC and NARAC assets. The primary purpose of the radionuclide lists is to use

them as a default starting point for NARAC and FRMAC calculations before field monitoring and laboratory analysis data become available.

MATERIALS AND METHODS

The uranium device parameters were selected to be generally consistent with the National Planning Scenario 1 for a nuclear detonation (DHS 2006). The specific key parameters used to estimate the fission and activation products are shown in Table 1. Although the radionuclide lists presented in this report were derived from a specific yield (i.e., 10 kilotons), these results can be scaled to any desired weapon yield.

Table 1. Key uranium IND parameters and scenario used in the development of the default fission and activation product radionuclide inventory.

Device Fuel	Yield	Height	Device Type	Underlying Surface	Internal Cladding Material
25 kg split 94% ^{235}U, 6% ^{238}U (by mass)	10 kilotons, all-fission	Surface burst	Simple gun type	Concrete and asphalt mix	Stainless steel

The Livermore Weapons Activation Code (LWAC) (Spriggs, et al. 2008) was used to develop a complete source term inventory of fission and neutron-activation products generated from the detonation of an IND using the selected device and environmental characteristics. LWAC uses fission product inventories calculated by the Oak Ridge Isotope Generation (ORIGEN) code using the latest version of the Evaluated Nuclear Data File (ENDF), ENDF/B-VII.0, that was available at the time of the analysis. LWAC typically generates source terms of over 1,000 nuclide isotopes from the fission of the nuclear fuel and the neutron activation of the underlying surface, surrounding air, nuclear device cladding and nuclear fuel. Because of the difficulty of assessing the dose from more than 1,000 radionuclides and their progeny over many different integration periods, a fast in-growth assumption was implemented to reduce the number of radionuclides to a more manageable number. Under the fast in-growth assumption radionuclides with half-lives less than 2.5 minutes were immediately transmuted into their progeny. The fast in-growth assumption was justified because the radionuclides with half-lives of less than a few minutes will essentially entirely decay into their progeny during the development and stabilization period of the nuclear cloud and subsequent atmospheric transport to the location chosen for this study. The ground-deposited areal activities of these short-lived radionuclides would be very low and contribute insignificant dose over the time periods of interest. Although the fast-ingrowth assumption artificially advanced the radioactive transmutation down the radionuclide decay chain by a few minutes, this has an insignificant effect on the final isotopic lists while permitting the analysis to be completed more quickly. After the fast in-growth assumption was implemented, the remaining inventory of approximately 650 radionuclides provided the radionuclide source strengths used by the NARAC's Lagrangian Operational Dispersion Integrator (LODI) transport and diffusion model (Nasstrom et al., 2007).

The LODI model used the initial radionuclide inventory output from the LWAC code to estimate the downwind areal activity (MBq m^{-2}) of each ground-deposited radionuclide at 1 hour after detonation. Under the meteorological assumptions, the airborne plume had passed and the deposition was complete at 1 hour post detonation at the analysis location selected 10 km downwind. The predicted areal depositions near the plume centerline at a location 10 km downwind were used for the detailed analyses described in this report. LODI uses an expanded form of the Bateman equation (Bateman 1910) that considers decay chain branching to calculate the time-dependent activity of the radionuclide decay chains. The Dose Coefficient Data File Package (DCFPAK) dose coefficients developed by Oak Ridge National Laboratory (Eckerman et al., 2008) and the default radiological assessment methods specified by the Federal Radiological Monitoring and Assessment Center's (FRMAC) Assessment Manual (SNL 2012) were used to assess the dose from the uranium-fueled IND radionuclides. This report utilized the DCFPAK dose coefficients based on the biokinetic and dosimetric models applied in Federal Guidance Report No. 13 (EPA 1999).

The effects of fractionation result in the differential separation and deposition of the refractory and volatile elements as the fallout material cools during its transportation downwind (Hicks 1982). The net effect is that the ground-deposited radionuclide mixture near ground zero may be different than ground-deposited mixture found at greater distances due to the physical separation and differential deposition of the refractory and volatile elements. Although the fractionation effects can be significant, they are difficult to predict and are not included in this analysis.

LODI assigns gravitational terminal fall velocities to the modeled particles based on an assigned particle size distribution appropriate for the release scenario. Under most circumstances LODI models gaseous radionuclides as having no particle size. However, LODI's nuclear detonation algorithms were designed to model both the larger "local fallout" particles as well as smaller particles that can be carried hundreds of kilometers downwind and require all modeled radionuclides to be assigned a non-zero particle size for determination of gravitational terminal fall velocity. The default activity-size and activity-height distributions are particle-size dependent. The total radionuclide activity of non-gaseous

radionuclides was distributed into three particle size fractions. One set of distributions applied to the smaller "respirable" particles (less than 10 microns in diameter), a second set applied to the "local fallout" particles (on the order of a several tens of microns in diameter), and a third set was applied to the larger "local fallout" particles (hundreds of microns in diameter). Gaseous radionuclides and their progeny were assigned particle sizes based on assumptions of the size of dirt and debris particles likely to provide the carrier material at the time the radionuclides decay into progeny that condense into a solid form within the cooling fireball.

The LODI model was used to take the first pass at evaluating the dose from the suite of approximately 650 radionuclides to identify the top-dose producing radionuclides and those that contribute insignificant dose over the 11 times phases shown in Table 2. From this analysis, 69 top dose-producing radionuclides that are included in Sandia National Laboratories' (SNL) DCFPAK database, were identified for further dose pathway analysis and ranking. Table 2 also shows the percent of the total dose from the entire fallout mixture that is included when only the top 69 dose producing radionuclides listed in Table 3 are considered. For example over the 6 – 24 hour time phase, approximately 94.1% percent of the total dose from all fallout radionuclides is accounted for by the 69 radionuclides in Table 3. Table 3 provides the source strength (activity) of the uranium-fueled IND radionuclides (MBq $10kt^{-1}$) at time = 0 hour (detonation) and their corresponding areal activities (MBq 10kt m^{-2}) at 1 hour post detonation and at a near-plume-centerline location 10 km downwind. Table 3 also provides the corresponding integrated air activities (MBq·s m^{-3}) of the respirable fraction and total (respirable and non-respirable) integrated air activities of the radionuclides at the selected location 10 km downwind. The entire plume had passed at the selected downwind location at 10 km at 1 hour, thereby ensuring that the calculated areal activities and integrated air activities in Table 3 represent the complete activities.

Table 2. Dose Integration Time Phases

Time Phase Number	Time Phase Start Time (hour)	Time Phase Duration (hour)	Time Phase End Time (hour)	Percent of total dose included by 69 top dose-producing radionuclides
1	0	24	24	92.4
2	0	96	96	92.5
3	0	8,760	8,760	92.7
4	6	24	30	94.1
5	6	96	102	94.3
6	12	24	36	94.9
7	12	96	108	94.1
8	24	24	48	94.7
9	24	96	120	94.4
10	24	8,760	8,784	94.0
11	8,760	8,760	17,520	94.3

Table 3. Uranium-fueled IND source strengths, integrated air and areal activities

Radio-nuclide number	Radio-nuclide	Source strength at t = 0 hour (MBq $10kt^{-1}$)	Integrated air activity of all activity per 10 kt (MBq·s m^{-3})	Integrated air activity of respirable fraction per 10 kt (MBq·s m^{-3})	Deposited activity per 10 kt (MBq m^{-2})
1	^{137m}Ba	$4.24x10^{+10}$	$5.07x10^{-01}$	$1.07x10^{-01}$	$2.02x10^{-01}$
2	^{140}Ba	$5.37x10^{+10}$	$3.66x10^{+02}$	$9.37x10^{+01}$	$1.77x10^{+02}$
3	^{141}Ba	$5.31x10^{+13}$	$8.40x10^{+04}$	$1.69x10^{+04}$	$1.81x10^{+04}$

4	^{142}Ba	$8.48\times10^{+13}$	$5.05\times10^{+04}$	$8.07\times10^{+03}$	$5.55\times10^{+03}$
5	^{141}Ce	$7.11\times10^{+05}$	$7.97\times10^{+00}$	$2.43\times10^{+00}$	$6.88\times10^{+00}$
6	^{143}Ce	$4.60\times10^{+08}$	$2.68\times10^{+03}$	$7.21\times10^{+02}$	$1.45\times10^{+03}$
7	^{144}Ce	$2.10\times10^{+09}$	$1.43\times10^{+01}$	$3.67\times10^{+00}$	$6.96\times10^{+00}$
8	^{58}Co	$4.54\times10^{+08}$	$3.25\times10^{+00}$	8.38×10^{-01}	$1.61\times10^{+00}$
9	^{58m}Co	$8.43\times10^{+10}$	$5.51\times10^{+02}$	$1.40\times10^{+02}$	$2.59\times10^{+02}$
10	^{134}Cs	$6.04\times10^{+05}$	4.77×10^{-03}	1.24×10^{-03}	2.43×10^{-03}
11	^{134m}Cs	$3.75\times10^{+09}$	$2.21\times10^{+01}$	$5.52\times10^{+00}$	$9.84\times10^{+00}$
12	^{137}Cs	$2.38\times10^{+06}$	4.42×10^{-01}	1.13×10^{-01}	2.14×10^{-01}
13	^{138}Cs	$2.60\times10^{+12}$	$1.09\times10^{+05}$	$2.71\times10^{+04}$	$4.26\times10^{+04}$
14	^{129}I	2.34×10^{-03}	2.00×10^{-09}	6.30×10^{-10}	2.00×10^{-09}
15	^{131}I	$6.81\times10^{+07}$	$9.74\times10^{+01}$	$2.91\times10^{+01}$	$7.51\times10^{+01}$
16	^{132}I	$2.15\times10^{+10}$	$3.40\times10^{+02}$	$9.35\times10^{+01}$	$2.08\times10^{+02}$
17	^{132m}I	$3.52\times10^{+10}$	$1.74\times10^{+02}$	$4.23\times10^{+01}$	$7.07\times10^{+01}$
18	^{133}I	$5.24\times10^{+10}$	$4.33\times10^{+03}$	$1.16\times10^{+03}$	$2.36\times10^{+03}$
19	^{134}I	$2.27\times10^{+12}$	$6.44\times10^{+04}$	$1.70\times10^{+04}$	$3.30\times10^{+04}$
20	^{135}I	$2.62\times10^{+12}$	$1.67\times10^{+04}$	$4.23\times10^{+03}$	$7.81\times10^{+03}$
21	^{88}Kr	$3.27\times10^{+12}$	$1.90\times10^{+04}$	$0.00\times10^{+00}$	$0.00\times10^{+00}$
22	^{140}La	$1.67\times10^{+08}$	$5.31\times10^{+00}$	$1.50\times10^{+00}$	$3.57\times10^{+00}$
23	^{141}La	$7.53\times10^{+09}$	$2.02\times10^{+04}$	$5.45\times10^{+03}$	$1.09\times10^{+04}$
24	^{142}La	$8.53\times10^{+10}$	$5.02\times10^{+04}$	$1.29\times10^{+04}$	$2.29\times10^{+04}$
25	^{143}La	$6.55\times10^{+13}$	$7.01\times10^{+04}$	$1.29\times10^{+04}$	$1.16\times10^{+04}$
26	^{54}Mn	$8.45\times10^{+07}$	5.77×10^{-01}	1.48×10^{-01}	2.80×10^{-01}
27	^{56}Mn	$7.65Ex10^{+12}$	$4.37\times10^{+04}$	$1.09\times10^{+04}$	$1.94\times10^{+04}$
28	^{99}Mo	$1.94\times10^{+08}$	$1.69\times10^{+03}$	$4.31\times10^{+02}$	$8.14\times10^{+02}$
29	^{101}Mo	$5.83\times10^{+13}$	$6.53\times10^{+04}$	$1.22\times10^{+04}$	$1.12\times10^{+04}$
30	^{95}Nb	$1.61\times10^{+05}$	2.81×10^{-02}	8.47×10^{-03}	2.31×10^{-02}
31	^{95m}Nb	$2.64\times10^{+05}$	3.66×10^{-03}	1.02×10^{-03}	2.40×10^{-03}
32	^{97}Nb	$3.27\times10^{+10}$	$2.25\times10^{+03}$	$6.32\times10^{+02}$	$1.45\times10^{+03}$
33	^{144}Pr	$6.49\times10^{+07}$	$1.34\times10^{+01}$	$3.52\times10^{+00}$	$6.81\times10^{+00}$
34	^{144m}Pr	$2.36\times10^{+09}$	7.57×10^{-01}	1.23×10^{-01}	1.48×10^{-01}
35	^{88}Rb	$4.89\times10^{+11}$	$1.64\times10^{+04}$	$4.34\times10^{+03}$	$8.47\times10^{+03}$
36	^{89}Rb	$3.98\times10^{+12}$	$6.91\times10^{+04}$	$1.32\times10^{+04}$	$1.24\times10^{+04}$
37	^{106}Rh	$1.44\times10^{+09}$	$1.43\times10^{+00}$	3.66×10^{-01}	6.92×10^{-01}
38	^{103}Ru	$9.96\times10^{+09}$	$6.80\times10^{+01}$	$1.74\times10^{+01}$	$3.30\times10^{+01}$

Radio-nuclide number	Radio-nuclide	Source strength at t = 0 hour (MBq $10kt^{-1}$)	Integrated air activity of all activity per 10 kt (MBq·s m^{-3})	Integrated air activity of respirable fraction per 10 kt (MBq·s m^{-3})	Deposited activity per 10 kt (MBq m^{-2})
39	^{106}Ru	$2.09 \times 10^{+08}$	$1.44 \times 10^{+00}$	3.67×10^{-01}	6.92×10^{-01}
40	^{128}Sb	$5.37 \times 10^{+09}$	$4.25 \times 10^{+02}$	$1.19 \times 10^{+02}$	$2.70 \times 10^{+02}$
41	^{128m}Sb	$2.45 \times 10^{+11}$	$1.40 \times 10^{+02}$	$2.20 \times 10^{+01}$	$1.49 \times 10^{+01}$
42	^{129}Sb	$6.85 \times 10^{+10}$	$3.49 \times 10^{+03}$	$8.86 \times 10^{+02}$	$1.62 \times 10^{+03}$
43	^{130}Sb	$3.49 \times 10^{+12}$	$1.28 \times 10^{+04}$	$2.96 \times 10^{+03}$	$4.33 \times 10^{+03}$
44	^{131}Sb	$2.10 \times 10^{+13}$	$4.44 \times 10^{+04}$	$9.47 \times 10^{+03}$	$1.14 \times 10^{+04}$
45	^{128}Sn	$1.44 \times 10^{+12}$	$6.23 \times 10^{+03}$	$1.49 \times 10^{+03}$	$2.37 \times 10^{+03}$
46	^{89}Sr	$5.90 \times 10^{+06}$	$5.29 \times 10^{+01}$	$1.45 \times 10^{+01}$	$2.99 \times 10^{+01}$
47	^{90}Sr	$4.11 \times 10^{+05}$	4.01×10^{-01}	1.02×10^{-01}	1.94×10^{-01}
48	^{91}Sr	$1.63 \times 10^{+12}$	$1.06 \times 10^{+04}$	$2.70 \times 10^{+03}$	$5.03 \times 10^{+03}$
49	^{92}Sr	$5.88 \times 10^{+12}$	$3.38 \times 10^{+04}$	$8.45 \times 10^{+03}$	$1.50 \times 10^{+04}$
50	^{99m}Tc	$1.43 \times 10^{+05}$	$1.08 \times 10^{+02}$	$3.13 \times 10^{+01}$	$7.77 \times 10^{+01}$
51	^{101}Tc	$3.00 \times 10^{+09}$	$1.12 \times 10^{+05}$	$2.55 \times 10^{+04}$	$3.15 \times 10^{+04}$
52	^{104}Tc	$2.04 \times 10^{+13}$	$3.24 \times 10^{+04}$	$6.53 \times 10^{+03}$	$6.96 \times 10^{+03}$
53	^{129}Te	$3.26 \times 10^{+09}$	$1.11 \times 10^{+03}$	$3.16 \times 10^{+02}$	$7.40 \times 10^{+02}$
54	^{129m}Te	$1.94 \times 10^{+07}$	1.34×10^{-01}	3.41×10^{-02}	6.44×10^{-02}
55	^{131}Te	$5.32 \times 10^{+11}$	$4.98 \times 10^{+04}$	$1.26 \times 10^{+04}$	$2.08 \times 10^{+04}$
56	^{131m}Te	$2.23 \times 10^{+10}$	$1.51 \times 10^{+02}$	$3.85 \times 10^{+01}$	$7.22 \times 10^{+01}$
57	^{132}Te	$3.96 \times 10^{+10}$	$1.13 \times 10^{+03}$	$2.89 \times 10^{+02}$	$5.44 \times 10^{+02}$
58	^{133}Te	$5.53 \times 10^{+13}$	$5.01 \times 10^{+04}$	$9.04 \times 10^{+03}$	$8.14 \times 10^{+03}$
59	^{133m}Te	$6.38 \times 10^{+12}$	$2.66 \times 10^{+04}$	$6.34 \times 10^{+03}$	$9.99 \times 10^{+03}$
60	^{134}Te	$2.57 \times 10^{+13}$	$9.13 \times 10^{+04}$	$2.13 \times 10^{+04}$	$3.15 \times 10^{+04}$
61	^{138}Xe	$6.93 \times 10^{+13}$	$7.28 \times 10^{+04}$	$0.00 \times 10^{+00}$	$0.00 \times 10^{+00}$
62	^{91}Y	$4.34 \times 10^{+05}$	$2.03 \times 10^{+00}$	5.98×10^{-01}	$1.57 \times 10^{+00}$
63	^{91m}Y	$7.45 \times 10^{+08}$	$2.66 \times 10^{+03}$	$7.49 \times 10^{+02}$	$1.70 \times 10^{+03}$
64	^{92}Y	$6.97 \times 10^{+09}$	$4.52 \times 10^{+03}$	$1.29 \times 10^{+03}$	$3.06 \times 10^{+03}$
65	^{93}Y	$2.61 \times 10^{+10}$	$1.06 \times 10^{+04}$	$2.75 \times 10^{+03}$	$5.20 \times 10^{+03}$
66	^{94}Y	$5.37 \times 10^{+13}$	$8.78 \times 10^{+04}$	$1.78 \times 10^{+04}$	$1.92 \times 10^{+04}$
67	^{95}Y	$9.76 \times 10^{+13}$	$5.44 \times 10^{+04}$	$8.55 \times 10^{+03}$	$5.70 \times 10^{+03}$
68	^{95}Zr	$4.80 \times 10^{+07}$	$6.87 \times 10^{+01}$	$1.82 \times 10^{+01}$	$3.56 \times 10^{+01}$
69	^{97}Zr	$9.81 \times 10^{+11}$	$6.52 \times 10^{+03}$	$1.66 \times 10^{+03}$	$3.12 \times 10^{+03}$

The Table 3 radionuclides were further analyzed to develop shorter lists (i.e., short-lists) of the top dose-producing radionuclides for each of the 11 time phases shown in Table 2 to reduce the number of radionuclides to a more manageable size for atmospheric dispersion modeling and radiological assessments. Each Table 3 radionuclide that was generated from the LWAC code and deposited on the ground by the LODI model was assumed in the subsequent dose assessment analysis to be a parent radionuclide and the radionuclide progeny were grown in over the various time phases. The dose from all progeny radionuclides in each decay chain was attributed to the parent radionuclide of each decay chain. For example, ^{140}La was deposited on the ground as a parent radionuclide and it is also produced by the transmutation of ^{140}Ba. The radiological dose from ^{140}La, as a parent radionuclide, was tracked separately from the radiological dose from ^{140}La formed by the transmutation of ^{140}Ba. The radiological dose from ^{140}La, as the progeny of ^{140}Ba, was added to the radiological dose attributed to the ^{140}Ba chain. Thus, the radiological dose attributed to the ^{140}Ba decay chain over each time phase also included the radiological dose from the ingrowth and transmutation of ^{140}La.

The Turbo FRMAC Assessment Software Package (SNL 2011) was used to analyze the radiological doses from the uranium-fueled IND radionuclides using the FRMAC's default radiological assessment methods specified in the FRMAC Assessment Manual (SNL 2012) and the DCFPAK dose coefficients (ORNL 2008). Analyses were performed to determine the relative dose contribution from each parent radionuclide and from their complete decay chain progeny over each time phase. The reader is referred to the FRMAC Assessment Manual for detailed descriptions of the radiological dose assessment methods used in this report (SNL 2012).

The total effective dose (TED) to the adult receptor located 10 km downwind was calculating using the biokinetic and dosimetric models applied in Federal Guidance Report No. 13 (EPA 1999). The adult receptor was assumed to remain outside, without respiratory protection and unshielded throughout the duration of each time phase. The dose pathways considered for time phases starting at 0 hour included 1) committed effective dose (CED) from inhalation of the airborne plume, 2) effective dose (ED) from external exposure (submersion) to the airborne plume, 3) CED from inhalation of resuspended material, and 4) ED from external exposure (groundshine) to the ground-deposited material. The dose pathways considered for time phases starting after 0 hour included 1) CED from inhalation of resuspended material and 2) ED from external exposure (groundshine) to the ground-deposited material.

Plume inhalation doses were calculated from the integrated air concentrations of the respirable fraction of each radionuclide and the air submersion doses were calculated from the integrated air concentrations of the total (respirable and non-respirable) fractions of each radionuclide. The time-dependent Maxwell/Anspaugh (Maxwell et al. 2011) resuspension model was used to predict the dose from the inhalation of resuspended material. The time-dependent Anspaugh weathering model (Anspaugh 2002) was used to predict the decrease in the external dose from the ground-deposited material as it was weathered deeper into the soil column.

The TED (all dose pathways) for each parent radionuclide and their progeny, if any, were determined over each of the 11 time phases using the default FRMAC methods described above. The Table 3 radionuclides were then ranked by the sum of the combined radiological dose from all dose pathways that they and their progeny produced over each of the 11 time phases.

RESULTS AND DISCUSSION

Tables A1 though A11 in Appendix A provide the detailed results of the rankings of the top dose-producing parent radionuclides for the uranium-fueled device, shown in Table 3, over each of the 11 Table 2 time phases. For time phases starting at time = 0 hour, the Appendix A tables show the percent of

the TED from each of the four dose pathways [i.e., CED from inhalation of the airborne plume, ED from external exposure (submersion) to the airborne plume, CED from inhalation of resuspended material, and ED from external exposure (groundshine) to the ground-deposited material] for each parent radionuclide and their progeny. For time phases starting after time = 0 hour, the Appendix A tables show the percent of the TED from each of two dose pathways [i.e., CED from inhalation of resuspended material and the ED from external exposure (groundshine) to the ground-deposited material] for each parent radionuclide and their progeny. The percentages of total dose values in Appendix A tables are based upon the TED produced by only the fission and neutron activation radionuclides included in Table 3. The total dose percentages do not consider the dose contributions from radionuclides excluded from this list of top dose-producers. As shown in Table 2, the 69 top dose-producing radionuclides used in these analyses may have excluded approximately 6-8% of the dose from the entire fallout inventory.

For example Table A1 indicates that the ^{134}Te chain produces 9.31% of the TED from all pathways and all radionuclides considered in the uranium-fueled device over the 0-24 hour time phase. Table A1 also shows that ^{134}Te chain produces 6.09% of the CED from the inhalation of radionuclides in the airborne plume, 4.01% of the ED from external exposure (submersion) from radionuclides in the airborne plume, 0.99% of the CED from the inhalation of resuspended material and 9.47% of the ED from groundshine over the 0-24 hour time phase. Furthermore, Table A1 shows that the top 18 dose-ranked radionuclides and their progeny produce 90.12% of the cumulative (i.e., dose from all radionuclides over the time phase) TED over the 0-24 hour time phase.

The Appendix A tables reveal that a relatively small number of parent radionuclides and their progeny deliver the majority of the TED over each of the time phases. The number of top-dose producing radionuclides decreases as the start of the dose integration period (time phase) is delayed further after time = 0 hour and as the length of the dose integration period increases. For example, from Table A1, the top 18 dose-producing parent radionuclides and their progeny deliver over 90% of the TED from the entire uranium-fueled IND source term investigated over the 0-24 hour time phase. As another example, from Table A10, the top 10 dose-producing parent radionuclides and their progeny deliver over 90% of the TED from the entire uranium-fueled IND source term investigated over the 1-366 day time phase.

Table 4 shows the number of parent radionuclides and their progeny that produce greater than 90% of the TED produced by the 69 parent radionuclides in Table 3 over each of the 11 time phases. For example, Table 4 shows that over the 0 – 24 hour time phase 18 parent radionuclides and their progeny produce over 90% of the TED from the 69 parent radionuclides in Table 3 and their progeny.

Table 4. Number of parent radionuclides contributing over 90% of TED from the 69 radionuclides listed in Table 3

Time Phase	No. of parent radionuclides producing over 90% of TED from the 69 radionuclides used in this analysis
0 - 24 Hour	18
0 - 96 Hour	19
0 - 365 Day	21
6 - 30 Hour	11
6 - 102 Hour	12
12 - 36 Hour	10
12 - 108 Hour	10
24 - 48 Hour	9

24 - 120 Hour	9
1 - 366 Day	10
366 - 731 Day	5

Table 5 summarizes the percentage of the TED that comes from the various dose pathways considered for the uranium-fueled IND and over each of the 11 time phases. Table 5 shows that the plume pathways (i.e., direct plume inhalation, external dose from air submersion) deliver < 3% of the TED received by adult receptors over the three time phases that start at time = 0 hour. Table 5 also shows that the dose from external exposure of the ground-deposited material (i.e., groundshine) typically accounts for at least 97% of the TED received by adult receptors over the individual time phases.

Table 5. Dose pathway analysis of uranium-fueled IND radionuclide mixtures

	Airborne plume pathways		Ground-deposited pathways		Inhalation and external dose breakdown	
Time phase	Percent of TED from plume inhalation	Percent of TED from external air submersion	Percent of TED from inhalation of resuspended material	Percent of TED from external groundshine	Percent of TED from inhalation of plume and resuspended material	Percent of TED from external exposure to plume and ground-deposited material
0-24 h	0.30%	2.61%	0.11%	96.98%	0.41%	99.59%
0-96 h	0.25%	2.21%	0.19%	97.35%	0.44%	99.56%
0-8760 h	0.19%	1.69%	0.27%	97.84%	0.46%	99.54%
6-30 h	NA	NA	0.28%	99.72%	NA	NA
6-102 h	NA	NA	0.41%	99.59%	NA	NA
12-36 h	NA	NA	0.37%	99.63%	NA	NA
12-108 h	NA	NA	0.51%	99.49%	NA	NA
1-2 d	NA	NA	0.50%	99.50%	NA	NA
1-5 d	NA	NA	0.64%	99.36%	NA	NA
1-366 d	NA	NA	0.56%	99.44%	NA	NA
365-730 d	NA	NA	0.01%	99.99%	NA	NA

Consolidated IND radionuclide short-lists for radiological assessments

In addition to developing lists of top dose-producing radionuclides, a further goal of this study is to develop one radionuclide superset-list for the uranium-fueled device that is suitable for performing radiological assessments over any desired time phase. This time-independent superset-list includes a sufficient number of radionuclides to provide accurate radiological assessments, and yet, is short enough to enable the radiological assessments to be performed over reasonable time periods. The Table 6 radionuclides are a subset of the Table 3 radionuclides, and provide the recommended radionuclide superset-list for the uranium-fueled IND. This superset-list is suitable for performing radiological assessments over any time period, and provides the estimated areal activity (MBq m^{-2}) and integrated air concentration (MBq·s m^{-3}) for each parent radionuclide included in the source term. The 44 parent radionuclides of Table 6 produce greater than 92% of the TED from the entire fallout inventory (i.e., all fission and activation products) received by a receptor located 10 km downwind over each of the 11 times phases investigated.

Table 6. Recommend uranium-fueled IND source strengths, integrated air and areal activities

Radio-nuclide number	Radio-nuclide	Source strength at t = 0 hour (MBq $10k^{-1}$)	Integrated air activity of all activity per 10 kt (MBq·s m^{-3})	Integrated air activity of respirable fraction per 10 kt (MBq·s m^{-3})	Deposited activity per 10 kt (MBq m^{-2})
1	^{140}Ba	$5.37x10^{+10}$	$3.66x10^{+02}$	$9.37x10^{+01}$	$1.77x10^{+02}$
2	^{141}Ba	$5.31x10^{+13}$	$8.40x10^{+04}$	$1.69x10^{+04}$	$1.81x10^{+04}$
3	^{142}Ba	$8.48x10^{+13}$	$5.05x10^{+04}$	$8.07x10^{+03}$	$5.55x10^{+03}$
4	^{141}Ce	$7.11x10^{+05}$	$7.97x10^{+00}$	$2.43x10^{+00}$	$6.88x10^{+00}$
5	^{143}Ce	$4.60x10^{+08}$	$2.68x10^{+03}$	$7.21x10^{+02}$	$1.45x10^{+03}$
6	^{144}Ce	$2.10x10^{+09}$	$1.43x10^{+01}$	$3.67x10^{+00}$	$6.96x10^{+00}$
7	^{58}Co	$4.54x10^{+08}$	$3.25x10^{+00}$	$8.38x10^{-01}$	$1.61x10^{+00}$
8	^{58m}Co	$8.43x10^{+10}$	$5.51x10^{+02}$	$1.40x10^{+02}$	$2.59x10^{+02}$
9	^{137}Cs	$2.38x10^{+06}$	$4.42x10^{-01}$	$1.13x10^{-01}$	$2.14x10^{-01}$
10	^{138}Cs	$2.60x10^{+12}$	$1.09x10^{+05}$	$2.71x10^{+04}$	$4.26x10^{+04}$
11	^{131}I	$6.81x10^{+07}$	$9.74x10^{+01}$	$2.91x10^{+01}$	$7.51x10^{+01}$
12	^{133}I	$5.24x10^{+10}$	$4.33x10^{+03}$	$1.16x10^{+03}$	$2.36x10^{+03}$
13	^{134}I	$2.27x10^{+12}$	$6.44x10^{+04}$	$1.70x10^{+04}$	$3.30x10^{+04}$
14	^{135}I	$2.62x10^{+12}$	$1.67x10^{+04}$	$4.23x10^{+03}$	$7.81x10^{+03}$
15	^{141}La	$7.53x10^{+09}$	$2.02x10^{+04}$	$5.45x10^{+03}$	$1.09x10^{+04}$
16	^{142}La	$8.53x10^{+10}$	$5.02x10^{+04}$	$1.29x10^{+04}$	$2.29x10^{+04}$
17	^{54}Mn	$8.45x10^{+07}$	$5.77x10^{-01}$	$1.48x10^{-01}$	$2.80x10^{-01}$
18	^{56}Mn	$7.65Ex10^{+12}$	$4.37x10^{+04}$	$1.09x10^{+04}$	$1.94x10^{+04}$
19	^{99}Mo	$1.94x10^{+08}$	$1.69x10^{+03}$	$4.31x10^{+02}$	$8.14x10^{+02}$
20	^{101}Mo	$5.83x10^{+13}$	$6.53x10^{+04}$	$1.22x10^{+04}$	$1.12x10^{+04}$
21	^{103}Ru	$9.96x10^{+09}$	$6.80x10^{+01}$	$1.74x10^{+01}$	$3.30x10^{+01}$
22	^{106}Ru	$2.09\ x10^{+08}$	$1.44x10^{+00}$	$3.67x10^{-01}$	$6.92x10^{-01}$
23	^{128}Sb	$5.37\ x10^{+09}$	$4.25x10^{+02}$	$1.19x10^{+02}$	$2.70x10^{+02}$
24	^{129}Sb	$6.85\ x10^{+10}$	$3.49x10^{+03}$	$8.86x10^{+02}$	$1.62x10^{+03}$
25	^{130}Sb	$3.49\ x10^{+12}$	$1.28x10^{+04}$	$2.96x10^{+03}$	$4.33x10^{+03}$
26	^{131}Sb	$2.10\ x10^{+13}$	$4.44x10^{+04}$	$9.47x10^{+03}$	$1.14x10^{+04}$
27	^{128}Sn	$1.44\ x10^{+12}$	$6.23x10^{+03}$	$1.49x10^{+03}$	$2.37x10^{+03}$
28	^{89}Sr	$5.90\ x10^{+06}$	$5.29x10^{+01}$	$1.45x10^{+01}$	$2.99x10^{+01}$
29	^{90}Sr	$4.11\ x10^{+05}$	$4.01x10^{-01}$	$1.02x10^{-01}$	$1.94x10^{-01}$
30	^{91}Sr	$1.63\ x10^{+12}$	$1.06x10^{+04}$	$2.70x10^{+03}$	$5.03x10^{+03}$
31	^{92}Sr	$5.88\ x10^{+12}$	$3.38x10^{+04}$	$8.45x10^{+03}$	$1.50x10^{+04}$
32	^{104}Tc	$2.04\ x10^{+13}$	$3.24x10^{+04}$	$6.53x10^{+03}$	$6.96x10^{+03}$
33	^{131}Te	$5.32\ x10^{+11}$	$4.98x10^{+04}$	$1.26x10^{+04}$	$2.08x10^{+04}$
34	^{131m}Te	$2.23\ x10^{+10}$	$1.51x10^{+02}$	$3.85x10^{+01}$	$7.22x10^{+01}$
35	^{132}Te	$3.96\ x10^{+10}$	$1.13x10^{+03}$	$2.89x10^{+02}$	$5.44x10^{+02}$
36	^{133}Te	$5.53\ x10^{+13}$	$5.01x10^{+04}$	$9.04x10^{+03}$	$8.14x10^{+03}$
37	^{133m}Te	$6.38\ x10^{+12}$	$2.66x10^{+04}$	$6.34x10^{+03}$	$9.99x10^{+03}$
38	^{134}Te	$2.57\ x10^{+13}$	$9.13x10^{+04}$	$2.13x10^{+04}$	$3.15x10^{+04}$

Table 6. Recommend uranium-fueled IND source strengths, integrated air and areal activities

Radio-nuclide number	Radio-nuclide	Source strength at t = 0 hour (MBq $10k^{-1}$)	Integrated air activity of all activity per 10 kt (MBq·s m^{-3})	Integrated air activity of respirable fraction per 10 kt (MBq·s m^{-3})	Deposited activity per 10 kt (MBq m^{-2})
39	^{92}Y	$6.97 \times 10^{+09}$	$4.52 \times 10^{+03}$	$1.29 \times 10^{+03}$	$3.06 \times 10^{+03}$
40	^{93}Y	$2.61 \times 10^{+10}$	$1.06 \times 10^{+04}$	$2.75 \times 10^{+03}$	$5.20 \times 10^{+03}$
41	^{94}Y	$5.37 \times 10^{+13}$	$8.78 \times 10^{+04}$	$1.78 \times 10^{+04}$	$1.92 \times 10^{+04}$
42	^{95}Y	$9.76 \times 10^{+13}$	$5.44 \times 10^{+04}$	$8.55 \times 10^{+03}$	$5.70 \times 10^{+03}$
43	^{95}Zr	$4.80 \times 10^{+07}$	$6.87 \times 10^{+01}$	$1.82 \times 10^{+01}$	$3.56 \times 10^{+01}$
44	^{97}Zr	$9.81 \times 10^{+11}$	$6.52 \times 10^{+03}$	$1.66 \times 10^{+03}$	$3.12 \times 10^{+03}$

If the radiological dose assessor desires to use the shorter time phase-specific lists, then the assessor should refer to the Appendix A radionuclide lists. The advantage of using the time phase-specific lists is that the number of radionuclides that need to be included in the radiological assessment may be considerably less than those in Table 6 and this will simplify and speed up the radiological assessment. For example if the assessor was assessing the dose consequences from a uranium-fueled device over the 8760-17,520 hour time phase, then they may choose to use the information in Table A11. This table indicates that the vast majority of the dose comes from less than 10 parent radionuclides. It is relatively simple to perform the radiological assessment of 10 parent radionuclides. The radiological dose assessor must use their professional judgment to determine how many radionuclides from Appendix A should be included in the radiological assessment for the time phase under consideration.

Radionuclides in addition to those in Table 6 may need to be included in the radiological assessment if the ingestion pathway is being assessed. The U.S. Food and Drug Administration (FDA) has provided recommended Derived Intervention Levels (DILs) for 24 radionuclides (e.g., ^{134}Cs, ^{129}I, ^{95}Nb, ^{91}Y) that indicate the contamination levels at which intervention (e.g., embargo) of radiologically contaminated food should be considered (FDA 1998). The FDA also provides a method to calculate the DIL for other radionuclides (FDA 1998). The FRMAC Assessment Manual provides methods to predict the areal activities at which food produced in the contaminated zone may exceed the DIL (SNL 2012).

Analysis of the external dose rates from the IND mixtures

Fig. 1 shows the predicted external dose rate at 1 meter above ground from the ground-deposited, uranium-fueled IND radionuclide mixture of Table 3 from the time of deposition (assumed to be 1 hour post detonation) to 50 hours. Fig. 1 shows the rapid decline of the dose rate from the ground-deposited radionuclides. Fig. 1 reveals that at 5 hour post deposition (i.e., 6 hour post detonation) the external dose rate of the uranium-fueled IND is < 10% of the dose rate at the time of deposition.

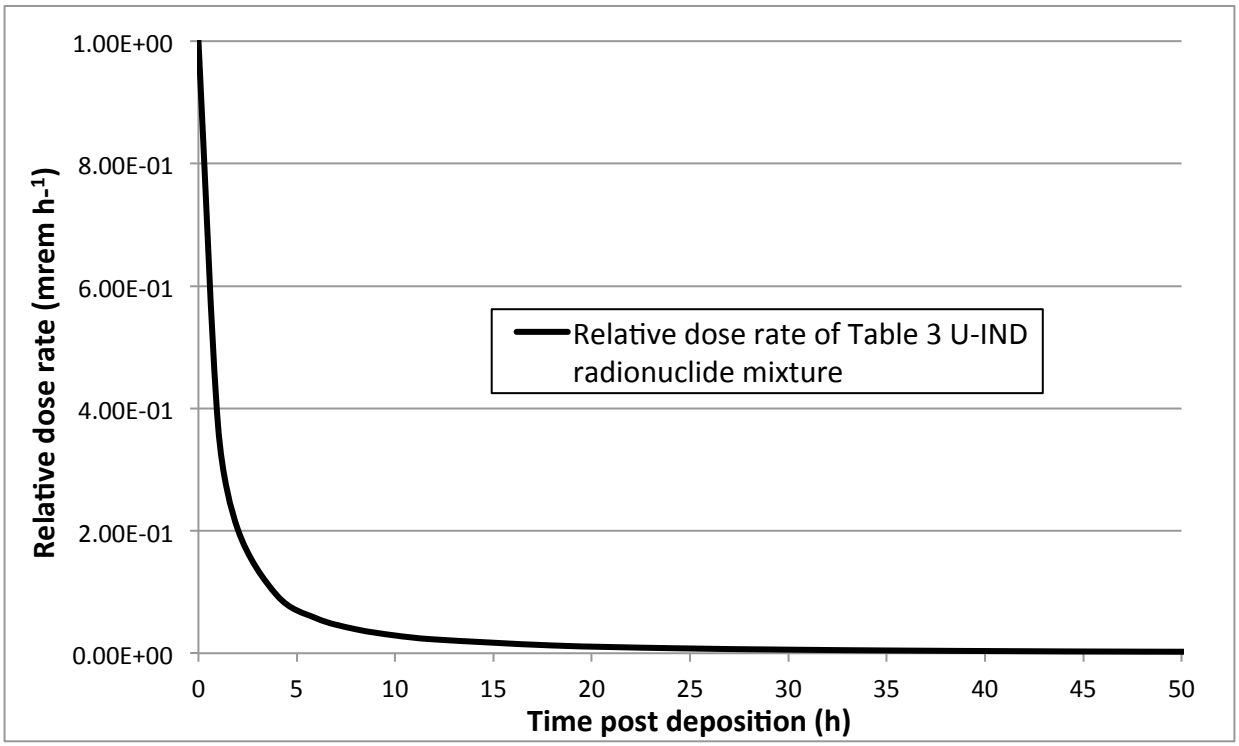

Fig. 1. Relative dose rate versus time for the Table 3 uranium-fueled IND fallout

The predicted dose rate versus time curve for the uranium-fueled IND was compared to the fallout decay curves described by Glasstone and Dolan (Glasstone 1977). Section 9.146 of this reference states that the dose rate from the fission and neutron-activation products is expected to decrease with time at a rate of ± 25% of $t^{-1.2}$, where t is in units of hours, for times from 30 minutes to about 200 days. The solid curve in Fig. 2 shows the calculated power function exponent (see left ordinate axis that shows the exponent x in the t^{-x} equation) of the changing dose rate of the Table 3 radionuclide mixture from 2 hours-200 days. The dashed curve in Fig. 2 shows the percent difference (see right ordinate axis) of the calculated dose rate power function exponent, x, of the Table 3 radionuclide mixture compared to the $t^{-1.2}$

power function exponent. Fig. 2 shows that the time-dependent change in the calculated dose rate of the uranium-fueled IND source term is in good agreement with that predicted by Glasstone and Dolan (Glasstone 1977). The calculated dose rates of the uranium-fueled IND over the first 15 days after deposition are approximately 15% greater than that predicted by the $t^{-1.2}$ power function. early (i.e., 1st 15 days) and the predicted dose rates from 15 – 200 days are generally less than 10% greater than the dose rate predicted by the $t^{-1.2}$ power function exponent.

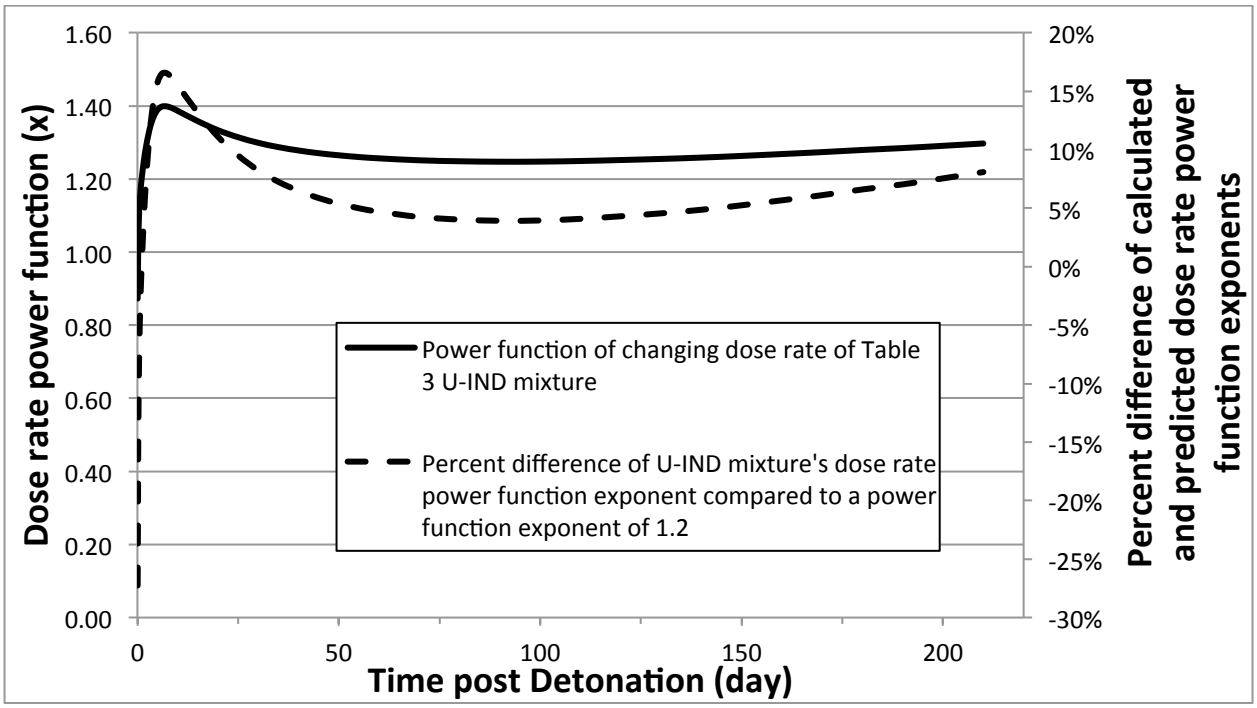

Fig. 2. Dose rate power function versus time, and percent difference of the calculated and predicted dose rate power functions for the Table 3 uranium-fueled IND radionuclide mixture

Fig. 3 compares the power function exponents of the dose rate from the uranium-fueled IND radionuclide mixtures of Table 3 (69 parent radionuclides) and Table 6 (44 parent radionuclides). Fig. 3 shows that the dose rates of the two mixtures change with time at nearly identical rates.

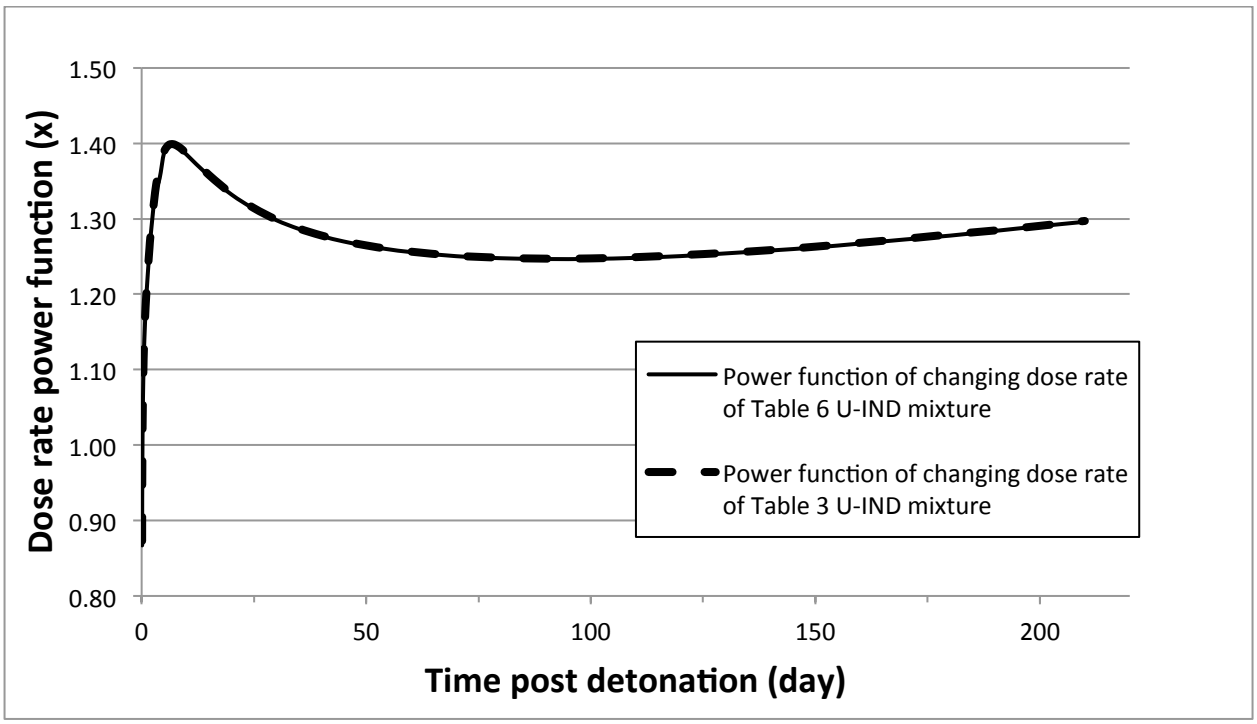

Fig. 3. Dose rate power function versus time of the calculated dose rate power functions for the Tables 3 and 6 uranium-fueled IND radionuclide mixtures

An analysis was performed to demonstrate how quickly the integrated ED from external exposure to the ground-deposited material is delivered by an IND radionuclide mixture that decays with a $t^{-1.2}$ power function exponent. The solid line in Fig. 4 shows the percent of the integrated (i.e., cumulative) ED delivered by an IND radionuclide mixture versus time over a dose integration period of 0.5 – 8760 hour. The dashed line in Fig. 4 shows the percent of the integrated ED delivered by the same IND radionuclide mixture versus time for a dose integration period of 10 – 8770 hour. The Fig. 4 abscissa is limited to 0 – 100 hours to highlight the percent of the integrated ED from external exposure delivered over the first 100 hours after deposition. Approximately 50% of the integrated ED delivered over a time phase of 0.5 – 8760 hours is delivered over the first 10 hours after the IND mixture has been deposited on the ground. However if the dose delivered over the first 10 hours is excluded from consideration, then it takes approximately 100 hours to accumulate 50% of the integrated ED delivered over a time phase of 10 – 8770 hours. Fig. 4 demonstrates the critical need to avoid or minimize exposure to the fallout over the first 10 hours or so. Public protection measures must quickly be initiated to move the public to sheltered locations or out of the fallout footprint to minimize the external exposure from ground-deposited materials.

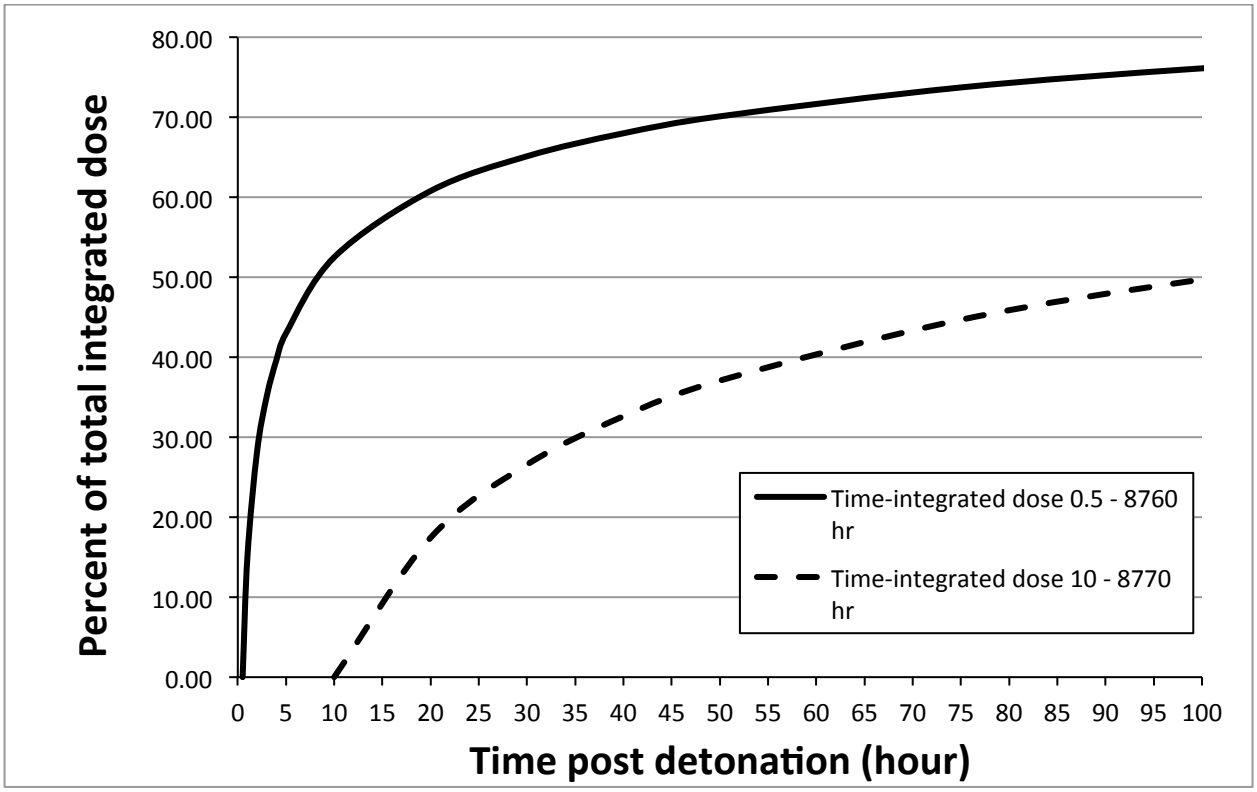

Fig. 4. Percent of time-integrated dose produced by external exposure to the fallout versus time for exposure periods of 0.5-8760 hours and 10-8770 hours

General considerations for radiological dose assessors

Radiological dose assessors should focus their efforts on providing sufficient radiological assessment data to decision makers to help them implement the appropriate protective actions. Early after a nuclear detonation radiological dose assessors will need to perform dose projections with little or no actual source term and device data. The actual areal activities of the IND fallout may be different than that discussed in this report due to many factors (e.g., IND characteristics, meteorological conditions, fractionation, particle size distribution) and may vary over the footprint of the fallout. Radiological dose assessors should work with sampling and monitoring personnel and laboratory analysis personnel to identify the areal activities of the top dose-producing radionuclides identified in this report. Atmospheric dispersion model predictions, such as from NARAC, can be adjusted using initial monitoring and sampling data to improve fallout model predictions in areas that have not yet been monitored and sampled.

Table 5 indicates that exposure to the airborne plume produces a very small portion of the TED over the time phase investigated in this study and under the assumed particle size distribution. However, the inhalation dose is very sensitive to the respirable fraction of the airborne material and the actual inhalation doses may vary accordingly.

In the absence of radiological source term data and device data, the radiological dose assessor can develop reasonable dose assessments using the power law function discussed by Glasstone and Dolan (Glasstone et al. 1977). Of course, this technique cannot account for the dose from the airborne plume material and can only account for the effective dose from external exposure to the ground-deposited radionuclides. A power law exponent of -1.2 is recommended if the actual power law exponent is not known. Radiological dose assessors should work with monitoring and sampling personnel to determine the actual power law exponent at various locations throughout the fallout footprint to ensure accurate dose assessments. The Table 6 radionuclide mixture will also provide reasonably accurate dose estimates that

are consistent with dose projections developed using the power law method and an exponent of -1.2. Radiological dose assessors should use the actual radionuclide mixture as soon as this data becomes available to ensure accurate radiological dose assessments.

CONCLUSIONS

This report analyzes the radiological dose delivered by the fission and neutron-activation products in fallout produced by a uranium-fueled IND detonation and identifies those radionuclides that produce significant dose over 11 different time phases. This report shows that a relatively small number of radionuclides produce the majority of the TED from the detonation of a uranium-fueled IND. The recommended radionuclide short-lists provide the radionuclide source terms that can be used to quickly and accurately assess the radiological consequences from the radioactive fallout produced by the detonation of a uranium-fueled IND. In the absence of device and radionuclide source term data, the power law function can be used to quickly provide a decay curve for dose estimates.

Sandia National Laboratories is a multi-program laboratory managed and operated by Sandia Corporation, a wholly owned subsidiary of Lockheed Martin Corporation, for the U.S. Department of Energy's National Nuclear Security Administration under contract DE-AC04-94AL85000.

This manuscript has been authored by Lawrence Livermore National Security, LLC under Contract No. DE-AC52-07NA27344 with the U.S. Department of Energy. The United States Government retains and the publisher, by accepting the article for publication, acknowledges that the United States Government retains a non-exclusive, paid-up, irrevocable, world-wide license to publish or reproduce the published form of this manuscript, or allow others to do so, for United States Government purposes.

REFERENCES

Anspaugh L. R., Simon S.L., Gordeev K.I., Likhtarev I.A., Maxwell R.M., Shinkarev S.M., Movement of Radionuclides in Terrestrial Ecosystems by Physical Processes, in *Health Physics*, Vol. 82, pp. 670-679, April 2002.

Bateman, H., Solution of a system of differential equations occurring in the theory of radioactive transformations, Proc. Cambridge Philos. Soc. 15 (1910), pp. 423-427. 1910.

Hicks, H. G., "Results of Calculations of External Gamma Radiation Exposure Rates from Fallout and the Related Radionuclide Compositions – the Trinity Event," Lawrence Livermore National Laboratory, UCRL-53705, December 1985.

Hicks, H. G., Calculation of the Concentration of Any Radionuclide Deposited On the Ground by Offsite Fallout from a Nuclear Detonation, in *Health Physics* Vol. 42, No,. 5 (May), pp. 585-600, 1982.

Eckerman K.F., Leggett R.W., Dose Coefficient Data File Package, Oak Ridge National Laboratory, 2008.

Glasstone S., Dolan P.J., The Effects of Nuclear Weapons, 3rd Edition. US Department of Defense, US Department of Energy, 1977.

Maxwell, R.M., Anspaugh, L.R., An Improved Model for Prediction of Resuspension. in *Health Physics*, Volume 101, pp. 722-730, December 2011.

Nasstrom, J. S., G. Sugiyama, R. L. Baskett, S. C. Larsen, M. M. Bradley, The NARAC modeling and decision support system for radiological and nuclear emergency preparedness and response, *Int. J. Emergency Management*, **4**, 525-550. 2007.

Sandia National Laboratories, "Turbo FRMAC Assessment Software Package," SNL, Albuquerque, NM, 2011.

Sandia National Laboratories, FRMAC Assessment Manual, Volume 1, Overview and Methods," SAND2012-0888P, SNL, Albuquerque, NM, June 2012.

Spriggs, G.D., V. Jodoin, J.R. Furlong, 2008, Livermore's Weapon Activation Code, LWAC: Quick Start User's Manual, Lawrence Livermore National Laboratory, UCRL-SM-229671-Rev 5, December 1, 2008. OUO/Export Controlled.

Sugiyama, Gayle; Nasstrom, John; Pobanz, Brenda; Foster, Kevin; Simpson, Matthew; Vogt, Phil; Aluzzi, Fernando; Homann, Steve (2012) Atmospheric Dispersion Modeling: Challenges of the Fukushima Daiichi Response, *Health Physics*, **102**, 493–508

U.S. Department of Homeland Security, National Planning Scenarios Created for Use in National, Federal, State, and Local Homeland Security Preparedness Activities, DHS, March 2006.

U.S. Department of Energy. Federal Radiological Monitoring and Assessment Center Operations Manual. DOE/NV /25946-980, U.S. Department of Energy National Nuclear Security Administration Nevada Site Office, May 2010.

U.S. Environmental Protection Agency. Manual of Protective Action Guides and Protective Actions for Nuclear Incidents, EPA 400-R-92-001. 1992.

U.S. Food and drug Administration, Accidental Radioactive Contamination of Human Foods and Animal Feeds: Recommendations for State and Local Agencies. Center for Devices and Radiological Health, FDFA, Washington, DC, August 13, 1998.

Footnotes:

*Terry Kraus
Sandia National Laboratories,
P.O. 5800, Mail Stop 0791,
Albuquerque, NM 87185-0791.

Email: tdkraus@sandia.gov
(505) 284-9708 - office
(505) 844-0708 - Fax

†Kevin Foster
Lawrence Livermore National Laboratory,
P.O. Box 808, L-103,
Livermore, CA 94551

Note to publisher: Mr. Foster has just retired from LLNL. Please direct all inquiries to Mr. Kraus